ISSN: 2502-4752, DOI: 10.11591/ijeecs.v40.i2.pp590-600

AlGaN/GaN MSM UV photodetector without and with BGaN back-barrier layer comparison study by SILVACO-TCAD

Aicha Benyettou, Abedelkader Hamdoune, Belkacem Benadda, Djamal Lachachi

Materials and Renewable Energy Research Unit, Department of Electrical and Electronic Engineering, Faculty of Technology, University of Abou-Bekr Belkaid, Tlemcen, Algeria

Article Info

Article history:

Received Oct 14, 2024 Revised Jun 24, 2025 Accepted Oct 14, 2025

Keywords:

Aluminum gallium nitride Boron gallium nitride Gallium nitride MSM photodetector UV photodetector

ABSTRACT

Using DevEDIT and atlas under SILVCAO-TCAD, we were able to achieve high photodetector metal-semiconductor-metal (MSM) AlGaN/GaN/BGaN performance with high electronic mobility. Our device demonstrated a sensitivity of 286 (I illumination/I dark) at Vanode 20V with an illumination current of 26 mA, a photocurrent of 1.56e-7 A at a wavelength of 0.350 μm , and an appropriate efficiency value of 87% without BGaN, and we also studied the influence of the boron B0.03Ga0.97N back-barrier layer. As a result, we obtain a sensitivity of 293,4 at Vanode 20V with an illumination current of 27 mA, a photocurrent of 1,85e-7 A at a wavelength of 0.350 μm , and an appropriate efficiency value of 90%. Additionally, this type of photodetector has been effectively created to detect UV light in the 100–450 nm range, and it may find value in both medical and military settings. Astronomical, medical diagnostics, environmental sensing, remote sensing, thermal imaging, optical signal detection, night vision cameras, missiles, and target tracking.

This is an open access article under the <u>CC BY-SA</u> license.



590

Corresponding Author:

Aicha Benyettou

Materials and Renewable Energy Research Unit, Department of Electrical and Electronic Engineering Faculty of Technology, University of Abou-Bekr Belkaid

Tlemcen BP 230 - 13000 Chetouane, Algeria

Email: canfience@gmail.com

1. INTRODUCTION

Recent research on high-quality devices using nitride III-V materials led to the realization of highperformance photodetectors in the UV spectral range. They have been acknowledged as a crucial technology for producing optical devices with high densities and low costs [1], and their significant uses in both the military and the civilian spheres have drawn increased attention. Nitrides have the advantage of wide and direct band gap, remarkable chemical stability, and good mechanical properties, which make them attractive for blue and UV light emitting, for high temperature, high power and high frequency electronic applications [2] Among these nitrides, boron nitride (BN) is a multiphase compound that has been investigated for many years and is employed in a wide range of industrial applications due to its remarkable electrical and structural characteristics, and have received more attention to their important applications in the military and civilian domains. They are used in defense warning systems, UV communication, space science, environmental monitoring, industrial production, medicine, and healthcare [3]-[7]. That allows building visible blind sensors and solar collectors [8]. They have many applications, such as chemical detection, flame detection, ozone hole detection, short-range communication, missile detection and guiding, monitoring vegetation growth, UV astronomy, and gas detection [9]-[11]. Metal-semiconductor-metal (MSM) photodiodes have gained popularity in the research community in recent years because of their basic benefits [12], [13]: a) easy to fabricate and integrate, b) simple construction, and c) minimal capacitance in relation to area.

Journal homepage: http://ijeecs.iaescore.com

MSM photodiodes are made up of two Schottky diodes arranged back-to-back on top of an active light collection area utilizing an interdigitated electrode design. This photodetector is unable to function in the absence of polarization because of its low capacity per unit of surface. MSM photodiodes are intrinsically fast and are generally limited by transit time rather than constant time. The size and spacing of electrodes may be achieved with a submicron dimension using electron beam lithography, which significantly improves speed. The main disadvantage of MSM photodetectors is their low intrinsic reactivity.

The photo responsibility of metal-semiconductor-metal detectors is low, owing to the fact that the oxidation of the electrodes casts a shadow across the active light collection region. The requirement for high-quality materials like AlN, GaN, BN, and their alloys, AlGaN, BGaN, in new technologies is critical. Fundamental research is critical for understanding growth mechanisms and hence improving material quality by controlling growth circumstances and exploring new avenues for putting contemporary growth capacity into practice [14]. The structure based on AlGaN/GaN materials has a number of interesting properties related to internal electrical fields caused by spontaneous and piezoelectric polarizations [15]. The field may be used to attract electrons, resulting in the development of a bidimensional (2D) electron gas in the canal layer [16].

Photodetectors based on AlxGa(1-x)N have the potential to be a significant detection technology in terms of cost, robustness, stability, power demand, and bandpass [17]. Due to a low capacity bearing and a high shunt resistance, MSM photodetectors made of SiC, GaN, or sapphire offer low noise, high speed, high sensitivity, and low polarization inverse. They can work invisibly on visible or infrared surfaces without interfering with other devices.

In the early 2000s, researchers worked to improve the performance of AlGaN UV photodetectors (PDs) by investigating new device topologies and material development methodologies [18]-[20]. The objective was to balance high sensitivity, low noise, rapid reaction time, and excellent quantum efficiency in the UV area. To overcome these issues, numerous research groups created novel device architectures, including Schottky photodiodes, avalanche photodiodes, and p-i-n photodiodes. These structures outperformed the MSM structure in terms of sensitivity, speed, noise reduction, and quantum efficiency [21]. The breakthroughs achieved in the 2000s set the groundwork for the development of AlGaN UV PDs with even greater performance in the following years.

MSM photodetectors using AlGaN/GaN/BGaN alloys have been the subject of extensive research in recent years, due to their exceptional performance in UV detection. A notable study is that of Pandit et al. (2023), who developed a highly sensitive UV photodetector based on an AlGaN/GaN HEMT structure with graphene electrodes on a p-GaN mesa structure. This design has significantly reduced the dark current and improved the sensitivity and detectivity of the device [22].

In addition, a simulation study by Allam *et al.* [23] optimized the design of GaN and InN/GaN/AlN-based MSM photodetectors for UV detection. The results showed a significant improvement in photocurrent and spectral responsivity in the UV region, suggesting that these structures can offer enhanced performance for UV detection applications. Furthermore, Vasallo *et al.* [24] studied the effect of adding a layer of BGaN to the photodetector structure. Their simulations demonstrated that increasing the boron concentration in the BGaN alloy improves optical absorption and generates a higher photocurrent in the UV range, making it a promising candidate for optoelectronic devices. This research illustrates significant advances in the development of UV photodetectors based on AlGaN/GaN/BGaN alloys, highlighting their potential for applications requiring efficient UV detection. Our paper presents a comprehensive exploration of large-area AlGaN/GaN MSM UV photodetector structures on sapphire wafers, aimed at investigating the elimination of crystal defects and reduction of dislocation density in the epitaxial MSM UV photodetector structure.

The primary objectives of this work are to fabricate MSM UV PDs using the selected structure and characterize their dark and photocurrents, responsivity, and specific detectivity, and to conduct optical simulations on AlGaN/GaN heterostructures with and without boron gallium nitride BGaN. Because boron has crucial chemical properties. This element has been extensively explored, both theoretically [25], [26] and practically [27], in various forms. Its stability and electrical characteristics were also investigated [28]. With their many intriguing characteristics, these new nanostructures have a wide range of potential applications in solar energy, photoconversion, batteries, sensors, nanoelectronics, and depth to identify the ideal shape for enhanced device performance. and to compare the performance of the simulation-patterned AlGaN/GaN MSM UV PDs to that of unpatterned devices.

This paper reports the successful development of a large-format UV with an Al-GaN/BGaN MSM photodetector by SILVACO-TCAD simulation; we obtain the principal characteristics. In this manuscript, we have simulated a metal-semiconductor-metal (MSM) AlGaN/GaN photodetector structure without and with a 3 µm thin layer of boron gallium nitride (BGaN) as a back-barrier layer for a 3% boron concentration. However, the growth of Bx Gax-1 N remains a challenge due to the large difference in atomic radius between boron and gallium [29]. Furthermore, it was shown that under normal growth circumstances, boron's solubility in GaN is restricted [30]. The objective of this study is to improve the performance of our device

and obtain a high-performance device with no interlayer dislocation and even better performance with the introduction of the BGaN back-barrier layer. In addition, this type of photodetector has been successfully developed to detect UV radiation in the 100 nm to 450 nm range and can be used in military and medical applications. Medical diagnostics, environmental sensing, remote sensing, optical signal detection, thermal imaging, night vision cameras, astronomy, missile tracking, target tracking, etc. The proposed structure could thus offer interesting prospects for the development of highly sensitive UV metal-semiconductor-metal photo-detectors, despite these advantages. Furthermore, the structure of BGaN may be less stable than that of GaN or AlGaN, especially at high boron concentrations. Finally, although the studies show significant improvements in performance, further research is needed to assess the long-term stability and reliability of devices using BGaN as a back-barrier layer.

2. METHOD

With 3D-DevEDIT, a sophisticated luminous 3D optical device simulator, in Figure 1, the AlGaN/GaN/BGaN MSM photodetector is shown in three dimensions: Figures 1(a) AlGaN/GaN MSM photodetector and Figure 1(b) AlGaN/GaN/BGaN/MSM photodetector.

It is necessary to select a refined meshing method for device meshing to obtain optimal results in Figure 2. Figures 2(a)-(d) show a 2D transverse section of our device, highlighting the various regions of AlGaN, GaN, and BGaN, with a luminous light source for the creation of 2DEG. Because photodetection in a semiconductor is based on or works with the general rule, it is the formation of electron-hole pairs under the action of light when photons have an energy equal to or less than the gap (Eg) of the semiconductor. The purpose of this paper is to model the electrical and optical characteristics of this diode and try to enhance them. This research will be based on the physical and optical characteristics of the materials employed, and it should result in the creation of efficient structures.

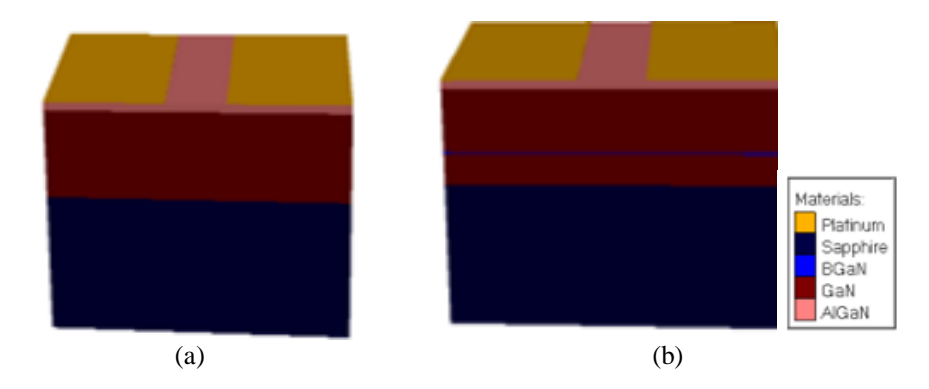


Figure 1. Schematic structure 3d of (a) AlGaN/GaN MSM photodetector and (b) AlGaN/GaN/BGaN/MSM photodetector

The ALGaN/GaN photodetector Figure 2(a) is produced on a c-plane sapphire substrate and consists of a 50 nm thick GaN buffer layer, a 100 nm thick GaN layer (doping n=1e16 cm³), an 8 nm thick Al0.25Ga0.75N nucleation area (doping N=1e16), and a 6 nm thick Al0.25Ga0.75N active layer (doping N=5e18 cm³). For the n-type Schottky contact, platinum metal (pt) electrodes with a thickness of 1 nm are used. This setup enhances the photosensitive surface while leaving the dynamic behavior the same. As a result, this planar structure, Al-GaN/BGaN MSM photodetector, which has a design similar to that of a field-effect transistor and a large bandwidth, makes it an ideal component for optoelectronic integrated circuits [31]. In Figure 2(b), we have the same structure, including, in addition, a 3nm-thick B0.03Ga0.99N layer between the n-GaN and GaN tanpon layer.

The proposed device structure was modeled and appropriately fine-meshed throughout the simulation by computationally solving the electron and hole continuity equations and the two-dimensional Poisson's equation in a finite number of points that comprise the mesh of the stated structure. The fundamental simulation parameters taken into account at $300 \, \text{K}^{\circ}$ are shown in Table 1 [32]-[36].

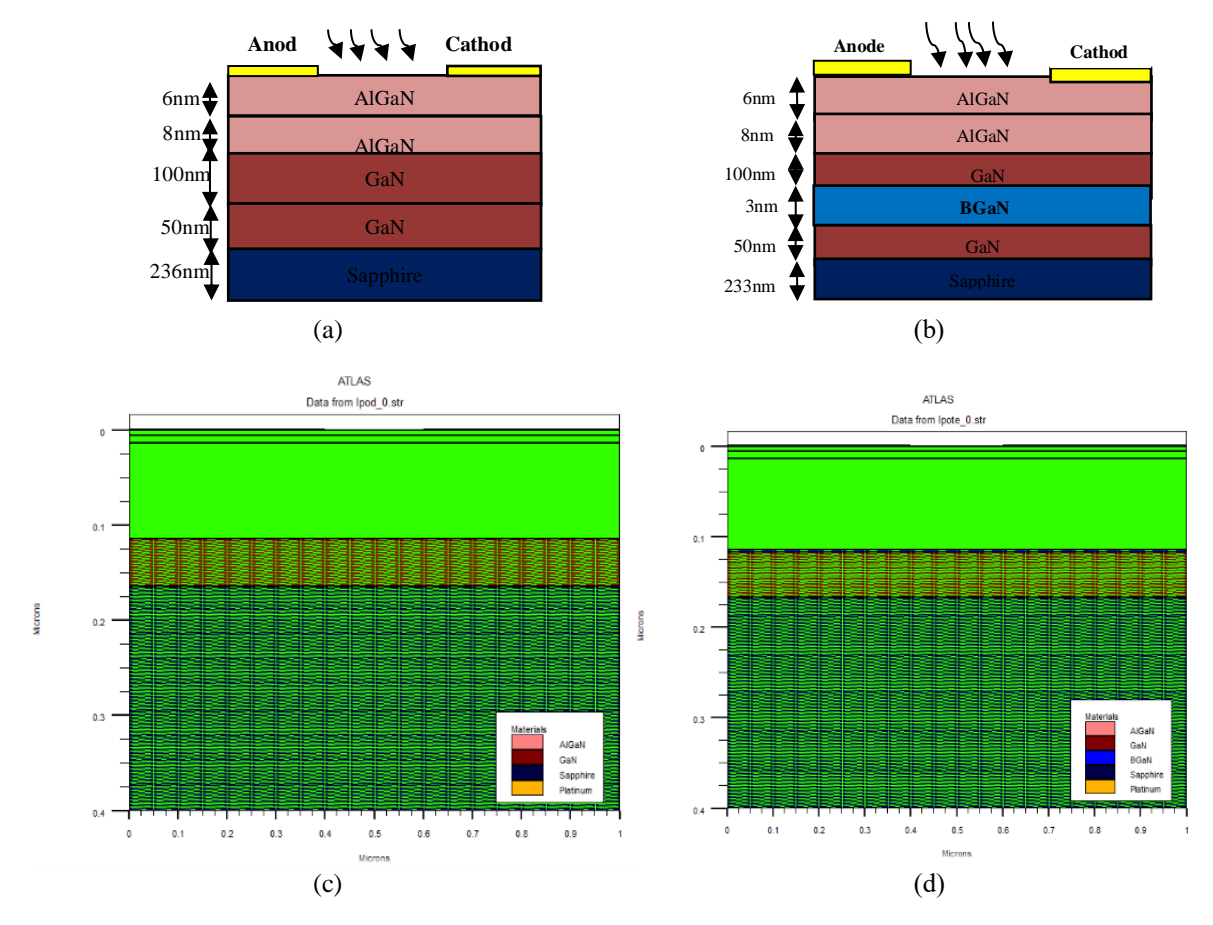


Figure 2. Schematic of the (a) AlGaN/GaN MSM photodetector, (b) AlGaN/GaN/B-GaN MSM photodetector, (c) meshing of the AlGaN/GaN MSM photodetector, and (d) meshing of the AlGaN/GaN/BGaN MSM photodetector

Table 1. The physical model parameters assumed at T=300 K

Parameters	Indication	GaN	AlXGaX-1N	BX GaX-1 N
Bandgap energy	Eg	3.4 eV	3.88eV	3.32eV
Material permittivity	εr	9,5	10.32	8.859
The carrier lifetimes of electrons	τn	1×10-9s	1× 10-9s	$5 \times 10 - 9s$
The carrier lifetimes of holes	au p	1×10-9s	1×10 -9s	5×10-12s
Mobility of electron	μe	900cm2/V s	600cm2/V s	50 cm2/V s
Mobility of hole	μh	10 cm2/V s	10 cm2/V s	40 cm2/V s
The electron affinity	χ	4.1	3.82	4.108
The electron density of states	Nc	1,08×1019 cm-3	2.07×1018 cm-3	2.96×1018cm-3
The hole density of states	Nv	1.16×1019cm-3	1.16×1019 cm-3	3.96×1018cm-3

3. RESULTS AND DISCUSSION

Figure 3 depicts the energy band diagram for an AlGaN/GaN in Figure 3(a) and an AlGaN/GaN/BGaN MSM photodetector in darkness and light in Figure 3(b). Numerical simulation is a very useful technique for investigating physical events in devices that influence electrical and optical properties. At room temperature, simulation results were achieved using Atlas Silvaco software and the Shockley-Read-Hall (SRH) model (300 K).

The energy band diagram was modeled utilizing BLAZE, which is interfaced with ATLAS. For III-V, II-VI, and devices with position-dependent band structures (heterojunctions), BLAZE is a versatile 2-D device simulator. Modifications to the charge transport equations in BLAZE accommodate the impacts of positionally dependent band structures. Two Schottky barriers linked back-to-back provide the fundamental building block of an MSM structure. The total of the two depletion widths rises in tandem with the applied voltage. The whole barrier's electron is far bigger than the barrier itself. The two depletion areas come into contact with one another at the reach-through voltage, Vrt, and the total precisely matches the flat band voltage, VFB. As the supplied voltage causes the effective hole barrier to fall, the hole current rapidly rises.

594 **I**SSN: 2502-4752

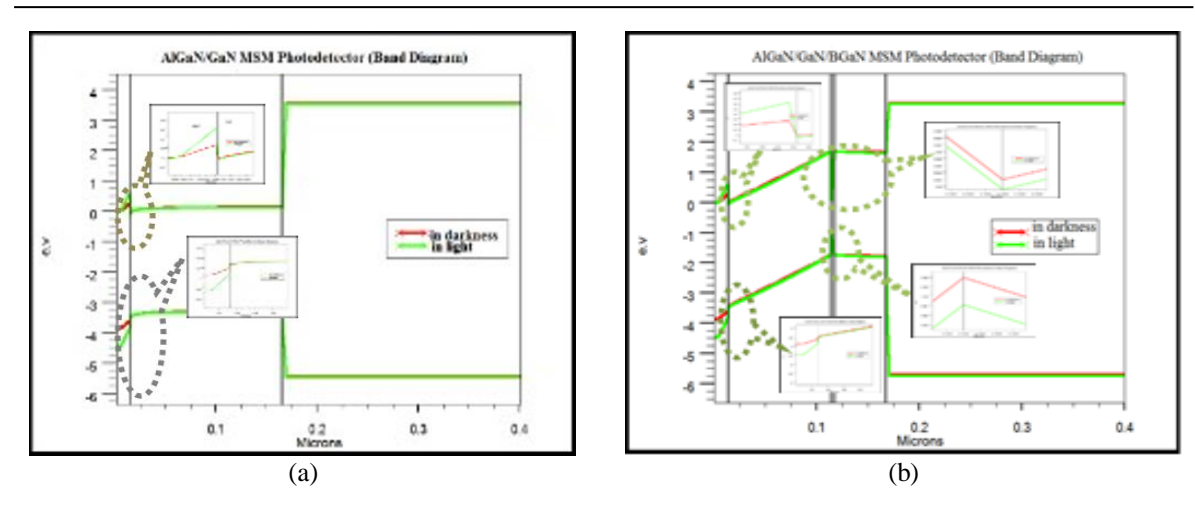


Figure 3. Band Diagram of (a) AlGaN/GaN MSM photodetector and (b) AlGaN/GaN/BGaN/MSM photodetector

Figure 4, shows the electrical-field MSM photodetector in dark and light conditions and without the BGaN. Without the BGaN layer, the electrical field at the interface of the layer that receives the illumination (AlGaN) increases from 2.94e5 V/cm in the dark to 6.88e5 V/cm in the light; however, when the BGaN layer was used, the electrical field increased to 3.01e5 V/cm in the dark and 6.93e5 V/cm in the light. Electromagnetic wave transmission analysis, or semiconductor analysis, may be used to analyze the energy flow across MSM photodetectors. P-i-n photodetectors and metal-semiconductor-metal (MSM) photodetectors both work on the same principles. Their reaction is connected to the current produced in the depletion area of two Schottky diodes by electron-hole pairs that are separated by an electric field. In this work, we used AlGaN alloy as the active layer because it is a direct band gap semiconductor and has high chemical resistance, high radiation resistance, and high gap energy, as shown in Figures 4(a) and (b).

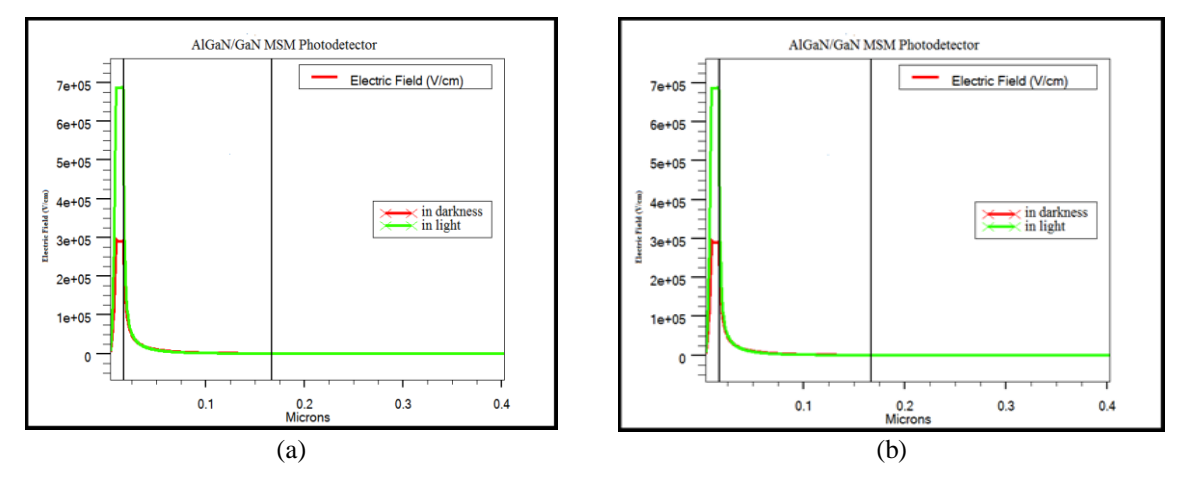
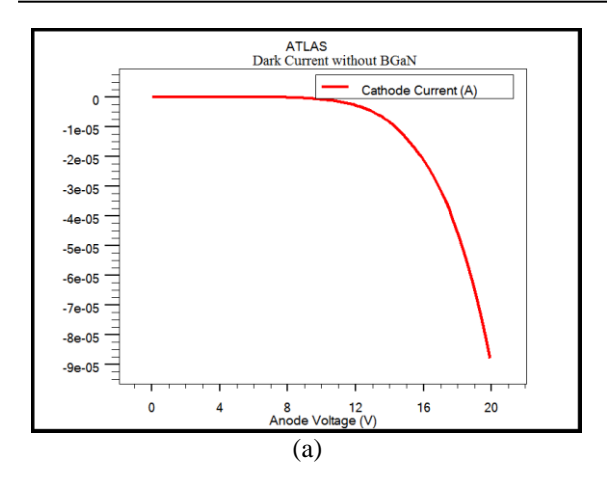


Figure 4. Electrical field of (a) AlGaN/GaN MSM photodetector and (b) AlGaN/GaN/BGaN MSM photodetector

Figure 5 shows the I-V property of the MSM photodetector in both dark and light environments, with and without BGaN. Figure 5(a) is without BGaN; we get 8.74e-5A in darkness and 2.6 mA in illumination at Vanode = 20 V; the sensitivity (I illumination/I dark) is 28.60. As a result, with BGaN, we have 9.2 e-5 A in the dark and 2.7 mA in illumination at Vanode = 20V, as shown in Figure 5(b). The sensitivity (I illumination/I dark) is 29.34. Due to the materials' efficient management of two-dimensional gas in the GaN channel and BGaN, this device is clearly a better option for photosensitivity applications as it has lower dark current and higher photosensitivity with and without BGaN. In Figure 6, we show the illumination currents in the MSM photodetector with and without BGaN.



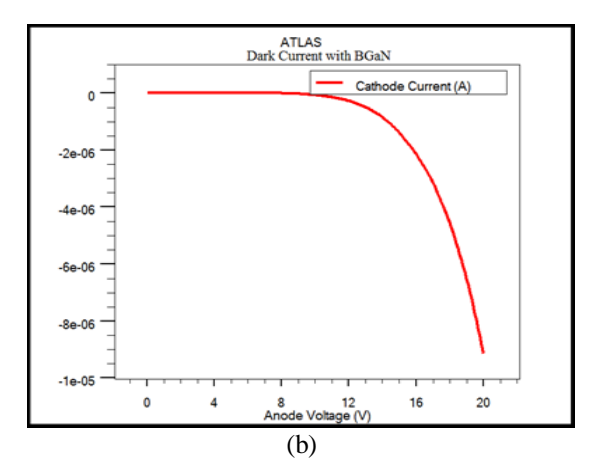


Figure 5. I-V characteristics of (a) AlGaN/GaN MSM photodetector and (b) AlGaN/GaN/BGaN/MSM photodetector in darkness

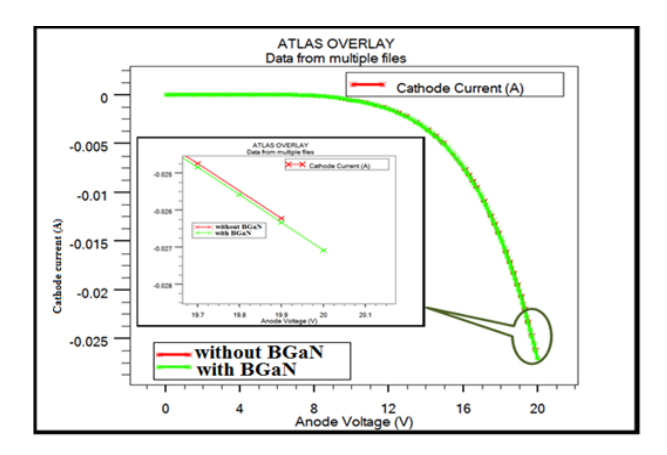


Figure 6. The illumination currents in the MSM photodetector UV with and without BGaN

The current that is produced as a result of photon absorption is known as photocurrent, also known as photogenerated current. Dark current is the current that exists when no light is impinged on the detector and is produced thermally or through phonon interaction. When light containing photons of a high enough energy strikes a semiconductor's surface, the photon may be absorbed, and electron-hole pairs may form. For a photon to absorb, occur, and move an electron from the valence band to the conduction band, its energy must be larger than or equal to the semiconductor material's band gap. The photon's energy can be linked to the light's wavelength or frequency, as illustrated by using a BGaN layer. The performance of a photodetector is determined by the dark current; the better if its value is small. The comparison of the Dark current/Photocurrent at a temperature of 300 K for a voltage of 20V of the photodetector with and without a layer of BGaN are shown in Table 2. For 3% boron concentration, we obtained a large increase in the layer resistivity; the dark current in the BGaN decreased.

In Figure 7, we illustrate that the available photocurrent is a function of wavelength. The maximum photocurrent is obtained at around $0.350~\mu m$ of incident light because the semiconductor absorbs the most light at this wavelength; we get 1.56e-7~A without BGaN and 1.85e-7~A with BGaN in the MSM UV Photodetector.

Table 2. Device's comparison in darkness and illumination current

Table 2. Device's comparison in darkness and illumination current					
Device	Dark current	Illumination current	Ref		
A study of BGaN/GaN Photo-detector UV/Blue	Between 10-4A and 10-3A	between 0.002A and 0.007A	[24]		
AlGaN/GaN MSM photodetector UV without BGaN	8.74e-5A	0.026A	This work		
AlGaN/GaN MSM photodetector UV without BGaN	9.2 e-5A	0.027A	This work		

596 □ ISSN: 2502-4752

$$E = hv = h * c/\lambda, \tag{1}$$

$$e \ photon = \frac{h \cdot c}{\lambda} oR \ h \cdot c = 1.24$$
 (2)

Eg AlGaN=3.88ev

$$\lambda = \frac{1.24}{ephoton}$$

$$\lambda = \frac{1.24}{3.88}$$

 $\lambda = 0.320 \mu m$

Where E is the energy of the photon, h is Planck's constant, ν is the optical frequency of the photon, c is the speed of light, and λ is the wavelength at which the lowest energy photon can be detected and whose energy is equal to the band gap.

In Figure 8, we show the optical response of the MSM UV photodetector with and without BGaN. We obtained a 19 A/W without BGaN and a 23 A/W with BGaN, with maximum responsivity at an optical wavelength of $0.350~\mu m$. The ratio of electrical output to optical input is the measure of a photodetector's sensitivity. Its definition is the ratio of incident optical power to photogenerated current. Reactivity is frequently expressed as amperes per watt, or volts per watt, in relation to incident radiant power. Both the wavelength of the incident light and the band gap of the material employed to create the photodetector affect responsiveness.

$$R = \eta \frac{e}{h\omega} = R_{max} = \eta \frac{\lambda[\mu m]}{1.24} \Longrightarrow \eta = \frac{R \times 1.24}{\lambda[\mu m]}$$
 (3)

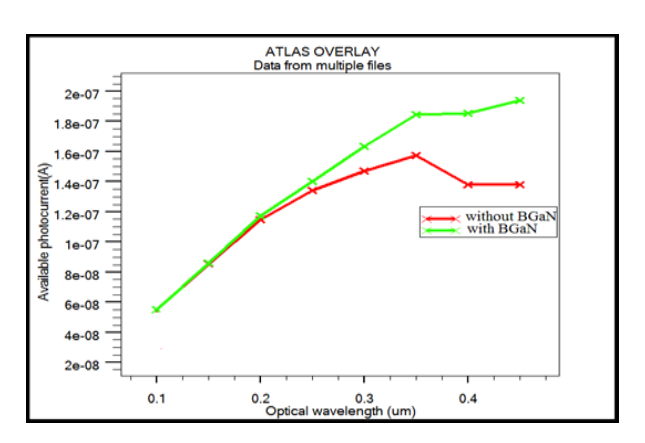


Figure 7. Spectral response of a UV MSM photodetector

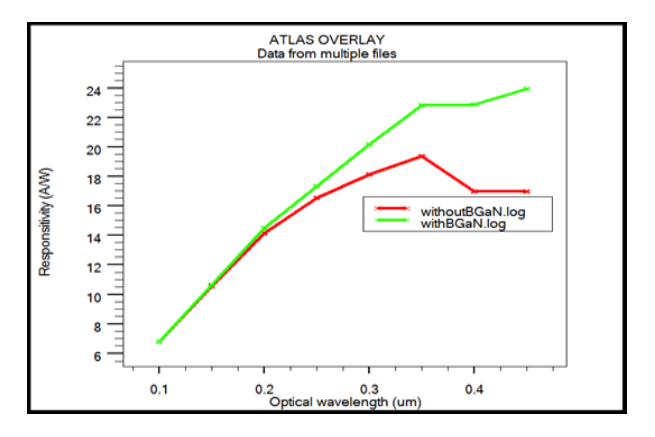


Figure 8. Responsivity of a UV MSM photodetector

In Figure 9, we show the quantum efficiency of the device. We obtained a η max of 88% without BGaN and 90% with BGaN, and at $\lambda = 0.350~\mu m$, we got a max of 68% without BGaN and 81% with BGaN. The device is able to detect mainly UV radiation. The quantum efficiency (η), which is the ratio of the number of electrons created to the number of photons impinging on the detector, is a crucial parameter for evaluating the detector's performance. In other terms, it is often stated in percentage units and may be described as the efficiency of converting a photon to an electron. A photodetector with a quantum efficiency of one would be perfect. The quantum efficiency of all photodetectors is really less than one.

Figure 10 illustrates the photodetector MSM UV's absorption and transmission in relation to the incident light's wavelength. The absorption may be expanded by using the alloys (Al, Ga, B) N; the detection threshold can be adjusted to collect the most photons while minimizing photon transmission. They are better than those of a photodetector without BGaN, which has a direct bearing on effectiveness. This has a direct impact on efficiency η . We obtained an absorption of 0.97 with BGaN and 0.88 without BGaN at $\lambda = 0.350$ μ m, as well as a transmission of 0.03 with BGaN and 0.12 without BGaN.

Figure 11 illustrates the capacitance as a function of the voltage with and without BGaN. The capacitance per unit area of the fully depleted semiconductor is equal to that of a parallel-plate capacitor. Two voltage ranges can be used to describe how an MSM structure's differential capacitance varies. The resulting capacitance per unit area when V<VRT is caused by two capacitances connected in series. The semiconductor is totally exhausted at V>VRT, and the capacitance per unit area is equal to that of a parallel-plate capacitor. Our device, in this context, the total capacitance per unit area comes from two depletion zones between the metal electrodes and the semiconductor i.e., two Schottky diodes in series.

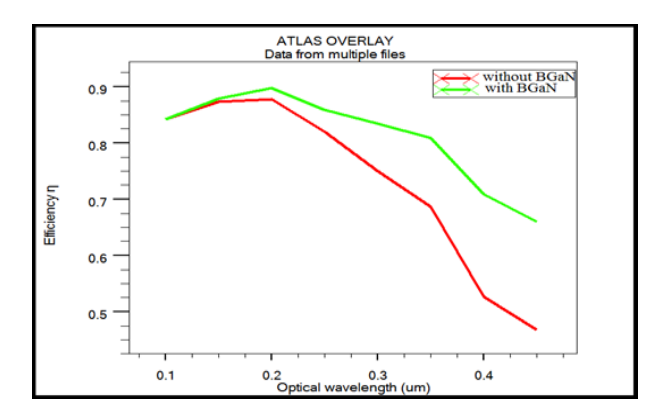


Figure 9. Efficiency of the UV MSM photodetector

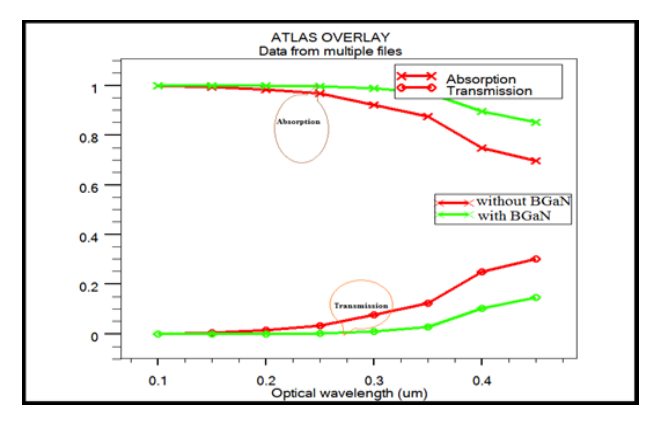


Figure 10. Absorption and transmission of a UV MSM photodetector

$$C_{MSM} = \frac{1}{c_1} + \frac{1}{c_2} \tag{4}$$

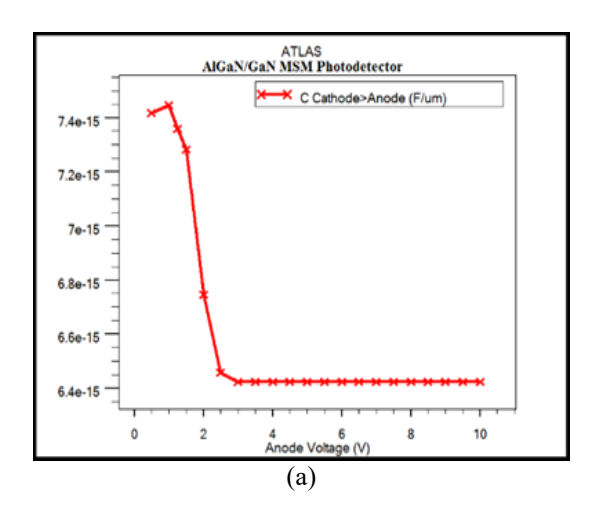
Our device has a planar and symmetrical structure, so C1=C2.

$$C_{MSM} = \frac{1}{2} \sqrt{\frac{\varepsilon q_S N_D}{2(V_{bi} + V)}} \tag{5}$$

598 □ ISSN: 2502-4752

Where q is the elementary charge, ε is the permittivity of the semiconductor, ND is the doping concentration (donor), Vbi is the built-in potential, and VRT is the Reaching Threshold Voltage. In Figures 11(a)-(b), we get with BGaN 7.49 e-15 F and without BGaN 7.44 e-15 F, which are low values indicative of low leakage current compared to what exists in the literature.

Figure 12 shows the speed of the MSM photodetector with and without BGaN. We analyze the rise-time response of our planar structure with and without BGaN. In the cathode current in 0V bias, i.e., solar cell mode, the transient response is analyzed because, with the bias voltage, the carriers drift faster, so we cannot predict the intrinsic transient behavior of the device. From Figures 12(a)-(b), we saw that the speed of the photodetector with and without BGaN is almost the same. We observe that our device has a fast transient response with and without BGaN. Our MSM photodetector with and without BGaN operates in the range of 1 e17 kHz with a photocurrent of 7.82 e-7 A. The photodetector speed is one of the main parameters to consider when evaluating the photodetector performance.



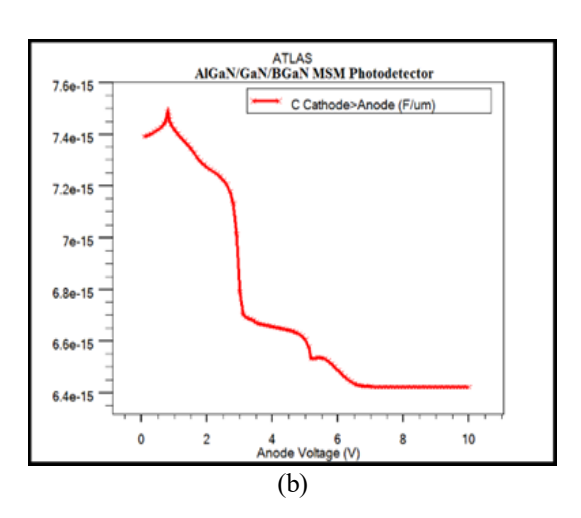
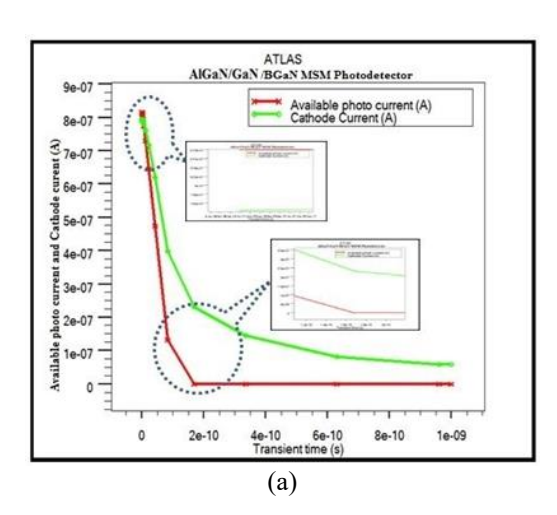


Figure 11. Capacitances of (a) without BGaN AlGaN/GaN MSM photodetector and (b) with BGaN AlGaN/GaN/BGaN/MSM photodetector



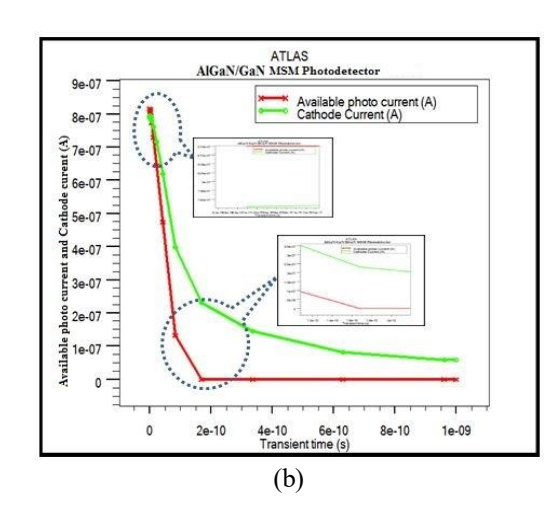


Figure 12. Transien response of (a) AlGaN/GaN MSM photodetector and (b) AlGaN/GaN/BGaN/MSM photodetector

4. CONCLUSION

A high-sensitivity illuminated AlGaN/GaN/BGaN MSM ultraviolet photodetector has been designed and characterized using the Silvaco simulator. The proposed photodetector exhibited a high efficiency η of 90% obtained by using a BGaN layer. However, because of the increased electrical field and high currents caused by the addition of BGaN, the rate of excess port recombination decreases. This gadget can be applied to a variety of UV-related applications. We obtained a high photocurrent equal to 26 mA and 27 mA with and

without BGaN, respectively, under illumination at 20V. The results show that the high-quality AlGaN/GaN/BGaN MSM photodetector UV structure proposed a device with low cost. This device can be

FUNDING INFORMATION

Authors state no funding involved.

CONFLICT OF INTEREST STATEMENT

used in different applications in the UV range.

Authors state no conflict of interest.

DATA AVAILABILITY

Data availability is not applicable to this paper as no new data were created or analyzed in this study.

ISSN: 2502-4752

REFERENCES

- [1] J. E. Bowers, et al., "Recent advances in silicon photonic integrated circuits," Proc. SPIE 9774, The International Society for Optical Engineering, vol. 977402, 2016, doi: 10.1117/12.2221943.
- [2] Tewfik. BAGHDADLI, "Study of the structural and electronic properties of new materials based on III-N alloys for optoelectronics," Thesis, Université de Lorraine, France, 2009.
- [3] E. Ozbay, N. Biyikli, I. Kimukin, T. Tut, T. Kartaloglu, and O. Aytur, "High-performance solar-blind photodetectors based on Al/sub x/Ga/sub 1-x/N heterostructures," *IEEE J. Quantum Electron*, 2004, 10-742.
- [4] N. Biyikli, I. Kimukin, T. Tut, O. Aytur, and E. Ozbay, "Solar-blind AlGaN-based Schottky photodiodes with low noise and high detectivity," Appl. Phys. Lett, vol. 81, no. 17, 2002, pp. 3272-3274, doi: 10.1063/1.1516856.
- [5] M. Razeghi and A. Rogalski, "Semiconductor ultraviolet detectors," J. Appl. Phys., vol. 79, no. 10, 1996, doi: 10.1063/1.362677.
- [6] R. W. Chuang, S. P. Chang, and S. J. Chang, "Gallium nitride metal-semiconductor-metal photodetectors prepared on silicon substrates," *Journal of Applied Physics*, vol. 102, no. 7, 2007, doi: 10.1063/1.2786111.
- [7] X. Li, et al., "Recent advances in avalanche photodiodes," IEEE J. Quantum Electron, vol 10, no. 4, 2004, pp. 777-787.
- [8] N. Biyikli, I. Kimukin, O. Aytur, M. Gokkavas, M. S. Unlu, and E. Ozbay, "High-speed visible-blind GaN-based indium-tin-oxide Schottky photodiodes," Appl. Phys. Lett, vol. 79, 2001, doi: 10.1063/1.1412592.
- [9] C. J. Collins, et al., "Improved devices performance using a semi-transparent p-contact AlGaN/GaN Heterojunction Positive-Intrinsic-Negative Photodiode," Appl. Phys. Lett, vol. 75, 1999, doi: 10.1063/1.124942.
- [10] T. Kashima, et al., "Microscopic Investigation of Al0.43Ga0.57N on Sapphire," Jpn. J. Appl. Phys, vol. 38, no. 12B, 1999, doi: 10.1143/JJAP.38.L1515.
- [11] E. Monroy, F. Omnes, and F. Calle, "Wide-bandgap semiconductor ultraviolet photodetectors," Sci. Technol, 2003, vol. 18, n0.4, doi: 10.1088/0268-1242/18/4/201.
- [12] G. W. Khan, et al., "In0.53Ga0.47As metal-semiconductor-metal photodiodes with ransparent cadmium tin oxide schottky contacts," Appl. Phys. Letts., vol. 65, 1930-1932, 1994.
- [13] Y. K. Su, et al., "GaN and InGaN metal-semiconductor-metal photodetectors with different Schottky contact metals," Jpn, J. Appl. Phys., 2001, vol. 40, 2001, pp. 2996-2999.
- [14] P. Masri, "Silicon carbide and silicon carbide-based structures, the physics of epitaxy," Surface Science Reports, vol. 48, 2002.
- [15] Mc. R. Clintock, K. Mayes, A, Hasan, D. Shiell, P. Kung, and M. Razeghi, "Avalanche multiplication in AlGaN based solar-blind photodetectors," *Applied Physics Letters*, 2005.
- [16] D. G. Zhao, et al., "Influence of defects in n--GaN layer on the responsivity of Schottky barrier ultraviolet photodetectors," Applied Physics Letters, vol. 90, no. 6, 2007.
- [17] J. C. Carrano, T. Li, P. A. Grudowski, R. D. Dupuis, and J. C. Campbell, "Improved detection of the invisible," *IEEE Circuits Devices Mag*, vol. 15, 1999.
- [18] K. Kishino, M. Yonemaru, A. Kikuchi, and Y. Toyoura, "Resonant-cavity-enhanced UV metal-semiconductor-metal (MSM) photodetectors based on AlGaN system," *Physica Status Solidi A Appl Res*, vol. 188, no. 1, pp. 321–324, doi: 10.1002/1521-396X(200111)188:1<321::AID-PSSA321>3.0.CO;2-8, 2001.
- [19] Y. Z. Chiou, Y. C. Lin, and C. K. Wang, "AlGaN photodetectors prepared on Si substrates," *IEEE Electron Device Letters*, vol. 28, no. 4, pp. 264–266, 2007, doi: 10.1109/LED.2007.893224.
- [20] S. J. Chang et al., "AlGaN ultraviolet metal-semiconductor-metal photodetectors grown on Si substrates," Sens Actuators A Phys, vol. 135, no. 2, pp. 502–506, 2007, doi: 10.1016/j.sna.2006.09.017.
- [21] S. Pandit, et al., "Development of a highly sensitive UV photodetector based on graphene electrode structure in AlGaN/GaN HEMT with p-GaN mesa configuration," Wiley Online Library, 2023, doi: 10.1002/admi.202202379.
- [22] A. Kilin, et al., "Optimization of MSM photodetector design based on GaN and InN/GaN/AIN for UV detection," arXiv, https://arxiv.org/abs/2503.14670, 2025.
- [23] M. Allam, et al., "Study of the effect of BGaN layer incorporation in photodetector structure: Optical absorption and photocurrent enhancement in the UV range," Taylor & Francis Online, 2024, doi: 10.1080/03772063.2024.2390091.
- [24] B. G. Vasallo, et al., "Monte carlo comparison between InP-Based double-gate and standard HEMTs," Proceedings of the 1st European Microwave Integrated Circuits Conference, Uk, 2006, pp. 304-307.
- [25] B. G. Vasallo, et al., "Comparison between the dynamic performance of double- and single-gate AlInAs/InGaAs HEMTs," *IEEE Trans on electron devices*, vol. 54, no. 11, 2007.
- [26] S. Zafar et al., "Designing of double gate HEMT in TCAD for THz applications," Proceedings of 2013 10th International Bhurban Conference on Applied Sciences & Technology (IBCAST), Islamabad, Pakistan, 2013.
- [27] S. R. Kumar, A. Mohanbabu, N. Mohankumar, and D. G. Raj, "Simulation of InGaAs Sub-channel DG-HEMTs for analog/RF applications," *International Journal of Electronics*, 2017, pp. 1-21.

600 ISSN: 2502-4752

[28] J. Jurkevičius, J. Mickevičius, A. Kadys, M. Kolenda, and G. Tamulaitis, "Photoluminescence efficiency of BGaN epitaxial layers with high boron content," *Phys. B Condens. Matter*, vol. 492, pp. 23–26, 2016, doi: 10.1016/j.physb.2016.03.033.

- [29] T. Honda, M. Shibata, M. Kurimoto, M. Tsubamoto, J. Yamamoto, and H. Kawanishi, "Band-gap energy and effective mass of BGaN," Japanese J. Appl. Physics, Part 1 Regul. Pap. Short Notes Rev. Pap., vol. 39, no. 4 B, 2000, doi: 10.1143/jjap.39.2389.
- [30] P. N. J. Dennis, "Photodetectors: An Introduction to Current Technology-Hardcover" Plenum Press, New York, 1986.
- [31] S. Poncé, D. Jena, and F. Giustino, "Route to high hole mobility in GaN via reversal of crystal-field splitting," *Phys. Rev. Lett.*, vol. 123, no. 9, pp. 1–6, 2019, doi: 10.1103/PhysRevLett.123.096602.
- [32] C. Boudaoud, A. Hamdoune, and Z. Allam, "Simulation and optimization of a tandem solar cell based on InGaN," *Math. Comput. Simul.*, vol. 167, 2020, doi: 10.1016/j.matcom.2018.09.007.
- [33] S. Sharma, A. Sumathi, and C. Periasamy, "Photodetection properties of ZnO/Si heterojunction diode: A simulation study," *IETE Tech. Rev.*, vol. 34, no. 1, pp. 83–90, 2017.
- [34] S. O. S. Hamady, T. Baghdadli, S. Gautier, M. Bouchaour, J. Martin, and A. Ougazzaden, "Raman scattering study of BxGa1-xN growth on AlN template substrate," *Phys. status solidi c*, vol. 5, no. 9, pp. 3051–3053, 2008.
- [35] S. Cornelius, M. Vinnichenko, N. Shevchenko, A. Rogozin, A. Kolitsch, and W. Möller, "Achieving high free electron mobility in ZnO: Al thin films grown by reactive pulsed magnetron sputtering," *Appl. Phys. Lett.*, vol. 94, no. 4, p. 42103, 2009.
- [36] Z. Allam, C. Boudaoud, A. M. Benahmed, and A. Soufi, "Simulation of the Electric Properties of a Structure Based on Two Gan P-N Junctions Grown on an Undoped ZnO Nanosheet," *International Conference in Artificial Intelligence in Renewable Energetic Systems*, 2020, pp. 946–957.

BIOGRAPHIES OF AUTHORS



Benyettou Aicha be solution obtained his master in electronic since 2015, and she has been a PHD student in Electronics (Materials and devices). Option: optoelectronics at the faculty of Technology, researcher in Research Unit of Materials and Renewable Energies, University of Abou-BekrBelkaid Tlemcen (Algeria). She can be contacted at email: canfience@gmail.com.



Hamdoune Abed Elkader botal solution by the sum of the



Belkacem Benadda works at the Department of Electrical and Electronics Engineering, Abou Bakr Belkaid University of Tlemcen. Belkacem does research in Telecommunications Engineering. Current work concerns the embedded solution development based on Software Defined Radio SDR Receivers and New Wireless Generations Systems. Hi had been a Professor (Assistant) since 2004 at the faculty of Technologie, He has been a professor in Telecommunications, since 2017. His research in Programmable logic FPGA, algorithms, data structure and object-oriented programming, networks and digital data transmission, computer architecture, assembly programming, embedded systems, computer and network security. He can be contacted at email: benadda.belkacem@gmail.com.



Djamal Lachachi received his master degree in electronics physics in 1990; and his Phd graduate in Telecommunications in 2017; he is a lecturer graduate in Electronics Engineering Department at Tlemcen University. His areas of interest include components of telecommunications, microelectronics components, industrial electronics and security; and renewable energy. He can be contacted at email: d_lachachi@yahoo.fr.